Biological activities of extracts from Aspidosperma subincanum Mart. and in silico prediction for inhibition of acetylcholinesterase

Biological activities of extracts from *Aspidosperma subincanum* Mart. and *in silico* prediction for inhibition of acetylcholinesterase

Bioassays of *A. subincanum* and prediction of AChE inhibition

Marina Pereira Rocha[1], Priscilla Rodrigues Valadares Campana[2], Denise de Oliveira Scoaris[2], Vera Lúcia de Almeida[2], Júlio César Dias Lopes[3], Andréia Fonseca Silva[4], Luc Pieters[5], Cláudia Gontijo Silva[1*]

[1]*Serviço de Biotecnologia Vegetal, Fundação Ezequiel Dias, Rua Conde Pereira Carneiro, 80, Belo Horizonte, CEP 30350-010, MG, Brasil;*

[2]*Serviço de Fitoquímica e Prospecção Farmacêutica, Fundação Ezequiel Dias, Rua Conde Pereira Carneiro, 80, Belo Horizonte, CEP 30350-010, MG, Brasil;*

[3]*NEQUIM, Departamento de Química, ICEx-UFMG, Av. Antônio Carlos 6627, Campus Pampulha, Belo Horizonte, CEP 31.270-901, MG, Brasil;*

[4]*Empresa de Pesquisa Agropecuária de Minas Gerais (EPAMIG), Av. José Cândido da Silveira, 1647, Belo Horizonte, CEP 31170-495, MG, Brasil;*

[5]*Natural Products & Food Research and Analysis (NatuRA), Department of Pharmaceutical Sciences, University of Antwerp, Belgium.*

e-mail: claudia.gontijo@funed.mg.gov.br

Phone: +55 31 3314 4791, +55 31 3314 4792

**Corresponding author*

ABSTRACT

Species of *Aspidosperma* are traditionally used to threat malaria, leishmaniasis, microbial and inflammatory diseases. *A. subincanum* Mart. known as "guatambu" is used in Brazilian traditional medicine to treat diabetes, hypercholesterolemia and digestive diseases. Its tonic properties have been employed by the indigenous populations to stimulate the circulatory and genitourinary tracts, and to improve respiratory function as well as to relieve spasms and to reduce fever. The species is known to contain antitumoural and antimalarial indole alkaloids. In the present study various less well explored biological activities of extracts from leaves and branches of *A. subincanum* were investigated, i.e. inhibition of acetylcholinesterase as well as antioxidant and antibacterial activity. Twenty one known indole alkaloids from this species were targeted for predicting the inhibition of acetylcholinesterase, and their biological activities were collected from the literature. Through *in silico* the prediction the indole alkaloids uleine and derivatives demonstrated a strong probability of being able to inhibit the acetylcholinesterase enzyme, as well as the olivacine derivatives 3,4-dihydroolivacine and N-methyl-tetrahydro-olivacine (guatambuine), and the subincanadines C and E. Indeed, the extracts of *A. subincanum* showed acetylcholinesterase inhibitory activity, antioxidant activity in the lipid peroxidation assay and antimicrobial activity against *S. aureus* ATCC 25923, and their pharmacological properties should be explored further.

Key words: *Aspidosperma subincanum* Mart., Apocynaceae, indole alkaloids, *in silico* prediction, biological activities, phytochemical characterization.

INTRODUCTION

The richness of the biodiversity of Brazil has awakened worldwide interest in the study of plants for their medicinal potential. Many of these plant species have been used since early times for the treatment of various diseases (Giraldi and Hanazaki, 2010). The search for new bioactive compounds from plant sources has contributed to the discovery and development of many drugs with therapeutic applications.

Alzheimer's disease (AD) is a progressive neurodegenerative disorder associated with a deficiency in cholinergic transmission, affecting the central nervous system (CNS). To date, only a few approved drugs are available for AD, the most common form of dementia and one of the most challenging diseases that affect the elderly populations. These drugs provide symptomatic relief in behavior and cognition in AD patients, although causing some undesirable side effects (Omar *et al*., 2017). There is a need for successful therapies to modulate the progression of the disease, which has a serious impact on both patients, and their families who provide long term care as well as being costly for health services worldwide.

Therefore, the search for new small molecules from natural sources capable of inhibiting AChE activity is particularly relevant. Many natural products have been shown to inhibit acetylcholinesterase (AChE) activity, as well as exhibiting antioxidant, anti-amyloid and anti-inflammatory activities, indicating promising new sources of alternatives for the treatment of AD (Bhaskar and Chintamaneni, 2014). Galantamine, an alkaloid isolated from *Galanthus nivalis* L., presents competitive, reversible and selective inhibitory activity of AChE and is one of the most frequently prescribed medications for the treatment of AD. Despite the fact that efforts have been made

towards the development of new synthetic drugs, plant extracts and their secondary metabolites are being investigated for their ability to inhibit AChE (Perry and Howes, 2011).

The Apocynaceae family is considered to be one of the most important sources of secondary metabolites, which are responsible for different biological activities relevant to the search and development of drugs. Several species of the genus *Aspidosperma* are traditionally used to threat malaria, leishmaniasis, microbial and inflammatory diseases (Brandão *et al*., 1992; TCA, 1995). The antimicrobial activity has been confirmed in vitro for some *Aspidosperma* species, such as, *A. ramiflorum*, which showed good activity against *Bacillus subtillis* and weak activity against *Staphylococcus aureus* (Oliveira *et al*., 2009). In addition, an extract from the roots of *A. tomentosum* was active against both *Candida krusei* LMGO 174 and *Cryptococcus neoformans* LMGO 02 (Albernaz *et al*., 2010).

Aspidosperma subincanum Mart. known as "guatambu" (Federlin *et al*., 2014) is used in Brazilian traditional medicine to treat diabetes, hypercholesterolemia and digestive diseases (Oliveira *et al*., 2009). Moreover, ethnobotanical data indicate that indigenous communities use a tonic prepared from its bark to stimulate the circulatory and genitourinary tracts, and to improve respiratory function as well as relieving spasms and reducing fever (Federlin *et al*., 2014).

Phytochemical studies of *A. subincanum* revealed the presence of indole alkaloids (Kobayashi *et al*., 2002; Pereira *et al*., 2007), which are nitrogenous substances with potent biological action. To date, over twenty alkaloids were isolated from this species, and some of them have shown antimalarial (Paula *et al*., 2014) and antitumoural activity

(Stiborová and Frei, 2015) (Fig. 1). Moreover, the alkaloid ellipticine (**6**) and its derivatives which have undergone under clinical trials as anticancer drugs (Cragg and Newman, 2005). There is an increasing interest in the potential of extracts, fractions and alkaloids of *A. subincanum* in order to provide insights for further studies targeting new lead compounds. This paper describes the evaluation of biological activities of extracts from the leaves and branches of *A. subincanum* for the inhibition of acetylcholinesterase as well as for antioxidant and antibacterial activity. In addition, known indole alkaloids from this species (Fig. 1) were targeted for predicting inhibition of AChE. Finally, the phytochemical characterization of the extracts was carried out based on their chromatographic profiles.

MATERIAL AND METHODS

Plant material

The leaves and branches of *A. subincanum* Mart. (Apocynaceae) were collected in São José de Almeida (S 19º 25' 834" W 43º 48' 506"), Minas Gerais, Brazil in 2008. The material was identified and a voucher specimen (PAMG 52460) was deposited in the Herbarium PAMG of the EPAMIG. This study received authorization for access and remittance of genetic material for scientific research by the CNPq (No. 010801/2015-4). The material was separated (leaves and branches) and subjected to drying in an oven with air circulation at 40 °C. After complete dehydration, the material was powdered and stored.

Preparation of extracts

Preparation of the ethanolic extract

The ethanolic extract was prepared with 10.0 g of powdered leaves and branches. The extractions were performed by sonication in an ultrasonic bath at 40 KHz using ethanol 92.8° (300 mL) for 10 min. The solution obtained was filtered and concentrated using a rotary evaporator. The process was repeated three times, and the combined extracts were dried (14.3% yield for leaves, 10.4% for branches), and stored at 4 ºC.

Preparation of alkaloid-enriched extract

For the preparation of an alkaloid-enriched extract a portion of 10.0 g of powdered leaves and branches was used. The plant material was moistened with a concentrated ammonium hydroxide solution and extracted with dichloromethane using a Soxhlet apparatus for 12 h. The solution obtained was concentrated in a rotary evaporator and the resulting alkaloid-enriched extracts were dried (7.0% yield for leaves, and 3.2% for branches), and stored at 4 ºC.

***In silico* prediction of anticholinesterase activity**

To perform the prediction of anticholinesterase activity, twenty-one indole alkaloids previously isolated from *A. subincanum* (Pereira *et al*., 2007) were selected (Fig. 1). There were five compounds with a uleine-like scaffold (**1-5**), nine with an ellipticine-olivacine-like scaffold (**6-14**) and seven subincadine derivatives (**15-21**). Seven compounds widely used as positive control for AchE inhibition (**22**-**28**) were also included in the prediction for comparison purposes. These alkaloids and reference compounds were submitted to two predictive anticholinesterase models generated using 3D structures of active and inactive compounds gathered from several datasets obtained

from the PubChem Bioassay database (Wang *et al*., 2017). Structural treatment, modeling and validation procedures, and how the predictions were performed are described below.

Dataset selection and pharmacophore fingerprint preparation

From the PubChem Bioassay database (Wang *et al*., 2017) we selected 1466 assays that hold AchE as the only biological target. The compounds tested within each unique assay identifier (AID) were filtered according to PUBCHEM_ACTIVITY_OUTCOME field in bioassay data file. We preserved only those classified as active or inactive, excluding those classified as inconclusive or unspecified. Furthermore, the compounds whose identifiers (CID) presented contradictory outcome among different assays were discarded. From the remaining compounds, we also excluded seven compounds used as positive controls in tests of inhibition of AChE (**22**-**28**). At the end we had a total of 4138 compounds associated to 628 assays, of which 3779 were active compounds and 359 inactive compounds. The list of all bioassay identifiers (AID) is provided as supplementary material.

As the number of active compounds largely exceeded inactive compounds we performed a clusterization of both sets to keep a more realistic proportion and, at the same time, eliminate redundancies while minimizing information loss. The clusterization used hashed chemical fingerprint (CF) and the Ward's minimum variance method (Ward, 1963) with JChem software from ChemAxon (JChem, 2016). The final dataset comprised a total of 400 representative compounds with 100 active compounds and 300 inactive compounds, which were downloaded from the PubChem Compound database using the 3D option with up to ten conformations each. A list of all compounds

identifiers (CID) is supplied as supplementary material allowing the model presented here to be replicated or compared with different modeling methods and procedures.

In-house software 3D-Pharma (Domingues, 2012) was used to convert the multi-conformational structures into 3-point pharmacophore fingerprints (Fig. 2). Each conformation of each compound was treated separately, and its heavy atoms were converted to potential pharmacophore points (PPP) which could be one or more of the following six types: hydrogen bond donor, hydrogen bond acceptor, positively charged, negatively charged, aromatic and lipophilic. All combinations of three pharmacophore points in the 3D space (triplets) were calculated to compose a pharmacophore fingerprint (Fig. 2). The union of uni-conformational fingerprints produce a unique modal fingerprint for each compound (Shemetulskis *et al*., 1996) which was used for all subsequent calculations.

Model building and validation with supervised machine learning methods SVM and Naïve Bayes

The multi-conformation (modal) pharmacophore fingerprint of active and inactive compounds were submitted to the in-house software ExCVBA (Santos *et al*., 2015) to build and validate machine learning models using a support vector machine (SVM) and the Naïve Bayes approach. The Naïve Bayes method is a probabilistic classifier based on Bayes' theorem that analyzes the frequency of descriptors in two sets with the aim of determining which class a new entry belongs to. Support vector machine (SVM) is a supervised learning method that recognizes patterns through the analysis of the descriptor space. A SVM model is a representation in a multi-dimensional space where

the instances in each category are divided by a hyperplane. When a new set of data is submitted to the SVM model it predicts whether it belongs to one or another group.

Each SVM or Naïve Bayes model was produced through a stratified random partition of the original dataset to produce two subsets, the first one being composed of 70% is the training set and the second being composed of 30% is the validation set (Fig. 3). This procedure was repeated 30 times and the average scores of each compound over the models in which it appears in the validation set was used to assess the modeling performance with the area under the ROC curve (AUC), as well for activity prediction of new compounds, as described below.

The SVM models were built with LibSVM (Chang and Lin, 2011) software and linear kernel option. The major parameter that affects the performance of a SVM classification model is the cost C which is a penalty parameter applied to misclassified compounds in the training data. The best value of C was selected with exponentially growing sequences from 2^{-12} to 2^{+6}, by means of a 5-fold cross-validation (CV) using the Power Metric (Lopes *et al*., 2017) at χ=0.5 as optimization objective metric to assure early recovery of active compounds. Additionally, we built a Naïve Bayes model using Perl module from CPAN repository (CPAN, 2017) which was incorporated into the ExCVBA software.

Prediction of anticholinesterase activity

In the prediction phase all studied indole alkaloids had their dominant tautomers and protonation states at pH 7.4 calculated by Chemaxon's Calculator Plugins (Marvin, 2016). Up to ten conformations were produced for each compound with OMEGA

software from OpenEye with standard options (Hawkins and Nicholls, 2012; Hawkins *et al*., 2010), which was the same software used to produce the conformations of PubChem compounds (Bolton *et al*., 2011).

The modal multi-conformational pharmacophore fingerprints of these compounds, produced as previously described, were submitted to all 30 SVM and Naïve Bayes models. The average scores were converted into probabilities through comparison with active and inactive compounds score distributions (validation set only) (Fig. 3), producing a measure of belonging to these two subsets (Filimonov *et al*., 2014).

Considering the average score of an unseen-compound as a reference or threshold value, the active probability (Pa) was estimated from the fraction of active compounds with worse scores, which is equal to false negative rate (FNR) (Equation 1). Similarly, the inactive probability (Pi) was estimated from the fraction of inactive compounds with better scores, which is equal to false positive rate (FPR) (Equation 2).

$$Pa = \frac{\mathrm{FN}}{N_a} = FNR \;\; and \;\; Pi = \frac{\mathrm{FP}}{N_i} = FPR \qquad \text{Eq. 1 and 2}$$

Where N_a and N_i are the number of active compounds and the number of inactive compounds; FN is the number of active compounds with worse scores than the threshold; and FP is the number of inactive compounds with better scores than the threshold. The difference between the Pa and Pi (Pa-Pi) was used to evaluate the potential anticholinesterase activity of modeled compounds (Fig. 3).

The variance of Pa-Pi (σ^2_{Pa-Pi}) was analytically calculated from the sum of variances of Pa and Pi (Equation 3) as proposed by Delong for the variance of AUC (Delong *et al*. 1988).

$$\sigma^2_{Pa-Pi} = \frac{var(Pa)}{N_a} + \frac{var(Pi)}{N_i} \quad \text{Eq. 3}$$

$$var(Pa) = \text{Pa} * (1 - \text{Pa}) \text{ and } var(Pi) = \text{Pi} * (1 - \text{Pi}) \quad \text{Eq. 4 and 5}$$

$$\sigma^2_{Pa-Pi} = \frac{\text{Pa} * (1 - \text{Pa})}{N_a} + \frac{\text{Pi} * (1 - \text{Pi})}{N_i} \quad \text{Eq. 6}$$

The confidence interval of Pa-Pi was calculated from the variance and Student t-value for a 95% confidence level (Equation 7) (Nicholls, 2014).

$$(\text{Pa} - \text{Pi})_{\text{estimate}} = (\text{Pa} - \text{Pi})_{mean} \pm t_{stat} * \sqrt{\sigma^2_{Pa-Pi}} \quad \text{Eq. 7}$$

Inhibition of acetylcholinesterase

Bioautographic assay

The evaluation of acetylcholinesterase (AChE) inhibitory activity of the extracts by thin-layer chromatography (TLC) was performed according to the methodology described by Marston *et al*. (2002). The assay was performed by preparing a reagent with Tris buffer (Tris [hydroxymethy] amino-methane) at pH approximately 7.8. The acetylcholinesterase enzyme (from electric eel, *Electropardus electricous* type VI-S) (Sigma-Aldrich, USA) was prepared by diluting 1000 U of the enzyme in 30 mL of Tris-HCl buffer (Tris [hydroxymethy] amino-methane) pH 7.8 with 30 mg of bovine serum albumin. The extracts (10 µL, 20 mg/mL) were applied onto a chromatographic silica gel 60 F_{254} plate (Merck, Germany) which was eluted with chloroform and methanol (9:1). The enzyme solution was sprayed and the air-dried plate was incubated in a humid chamber at 37 °C for 20 min. Detection was performed by spraying the plate with a solution of 1-naphthyl acetate (2.5 mg/mL) and Fast Blue B salt (2.5 mg/mL).

The anticholinesterase activity was indicated by the presence of white spots on a purple background after 5 min. Physostigmine (Eserine, Sigma-Aldrich, Switzerland) was used as the reference compound.

Microplate assay

AChE inhibitory activity was measured using a modified microplate assay based on Ellman's method (1961). The enzyme stock solution (AChE from electric eel, *Electropardus electricous* type VI-S, 2000 U/mL) (Sigma-Aldrich, USA) was prepared in Tris/HCl buffer (50 mM, pH 8.0), and kept at -20 °C. Further enzyme-dilution was done in 0.1% BSA in Tris/HCl buffer. DTNB was dissolved in Tris/HCl buffer (50 mM, pH 8.0) containing NaCl (10 mM) and $MgCl_2$ (20 mM). Acetylthiocholine iodide (ATCI, Sigma-Aldrich, USA) was dissolved in deionized water (14 mM). To perform the assay, 25 µL of test samples (400 µg/mL) of diluent, 50 µL of 0.1% BSA in Tris/HCl buffer, 125 µL of DTNB solution (3 mM), and 25 µl of ATCI were added to a 96-well microplate. The absorbance was recorded at 405 nm for background measurement. The enzymatic reaction was initiated by the addition of 25 µL of 0.2 U/mL of AChE. After mixing, the absorbance was measured at 405 nm in a Multiskan Go (Thermo-Fisher, USA) microplate reader and the readings were recorded every 5 min for 25 min. Physostigmine (Sigma-Aldrich, Switzerland) and galantamine (Sigma-Aldrich, USA) were used as the positive controls. The assay was performed in triplicate. The percentage inhibition was calculated according to Eq. 8.

$$Percentage\ inhibition = \frac{a - b}{a}\ x\ 100 \qquad \text{Eq. 8}$$

where a = ΔA/min of control; b= ΔA/min of test sample; ΔA= change in absorbance.

For this study, the IC_{50} value was determined for the extracts at concentrations of 25 µg/mL, 50 µg/mL, 100 µg/mL, 200 µg/mL and 400 µg/mL, and the assay was performed as aforementioned. The extracts showing an inhibition of AChE greater than 40%, were considered promising.

Evaluation of antioxidant activity

***β*-Carotene / linoleic acid co-oxidation assay**

The antioxidant activity using the β-carotene / linoleic acid co-oxidation system was performed as described by Duarte-Almeida *et al*. (2006), with modifications. Briefly, the extracts were solubilized in methanol obtaining an 2.2 mg/mL. Then, serial dilutions were done in methanol to give concentrations ranging from 3.125 to 200 µg/mL. A β-carotene solution was prepared in chloroform at 1.0 mg/mL. A portion of this solution (1.0 mL) was added to 25 mg of linoleic acid and 100 mg of Tween 40. The chloroform was evaporated under reduced pressure without heating. Aerated distilled water (50 mL) was added to the mixture. A blank emulsion was prepared as described above but without adding the β-carotene solution. The assay was carried out by transferring 25 µL of the test samples to of a 96-well plate, followed by the addition of 250 µL of either β-carotene (reaction wells) or blank emulsion (blank reaction wells). Quercetin and rutin were used as positive controls (20 µg/mL), and methanol was used as a blank. The absorbance was immediately recorded at 470 nm. After the first reading, the plate was incubated at 45 ºC and the absorbance was recorded every 15 min for 2 h. The antioxidant activity was expressed as % of inhibition of lipid peroxidation (%I), using the formula (I% = Ac (initial abs - final abs) - Aam (final abs -

initial abs) / Ac x 100). Assays were performed in triplicate and IC_{50} values were determined by non-linear regression using GraphPad Prism, version 6.0.

DPPH assay

The DPPH (1,1-diphenyl-2-picrylhydrazyl) radical has a purple color in its radical form, but in the presence of compounds capable of reducing this radical by donating an electron, the color changes to yellow. Antioxidant activity against the DPPH radical was performed according to Mensor *et al*. (2001) with modifications. Briefly, 250 µL of sample solutions (1.0 - 200 µg/mL) or 250 µL of the standard (positive control) or 250 µL of the sample diluent (negative control) were added to the wells of a microplate. Then, 100 µL of 300 µM ethanolic solution of DPPH was added. The absorbance was recorded every 5 min, for 45 min, at 515 nm, using a microplate reader (EL808IU-Biotek model). Pyrogallol (Sigma-Aldrich, USA, 50 µg/mL) was used as antioxidant standard. The percentage of radical scavenging activity (%RSA) was calculated by the following equation:

$$\%RSA = ((A_C - A_S)/A_C) \times 100 \qquad \text{Eq. 9}$$

where A_C is the absorbance of control recorded after 35 min, and A_S is the absorbance of samples recorded after 35 min.

A calibration curve was obtained weekly with different concentrations of DPPH (6.0 to 100 µg/mL) and this curve was used to calculate the residual concentration of DPPH in each well. The EC_{50} values were determined using non-linear regression of the curves obtained by plotting % of remaining DPPH *versus* concentration. The EC_{50} value

denotes the concentration of the sample required to scavenge 50% of the initial DPPH free radicals.

Evaluation of antibacterial activity

Susceptibility tests against *Staphylococcus aureus* ATCC 25923 and *Escherichia coli* ATCC 11775 were performed using a modified version of the methods for bacteria (CLSI, 2003). The extracts solubilized in DMSO at 50 mg/mL were diluted in Mueller Hinton Broth (MHB) at a concentration of 2.0 mg/mL. The bacterial isolates were grown in Mueller Hinton Agar (MHA) plates at 37 °C for 18-24 h. Then, the inoculum was adjusted in saline solution using a spectrophotometer at 625 nm to a concentration of 1-5 x 10^8 CFU/mL, and then diluted in MHB at a concentration of 1-5 x 10^5 CFU/mL. Volumes of 100 µL of the inoculum were added to the three wells containing 100 µL of the extracts at 2.0 mg/mL, in triplicate (one well intended for extract control), resulting in a final concentration of 1.0 mg/mL. Chloramphenicol at 100 µg/mL and 0.2% DMSO were used as positive and negative controls, respectively. Evaluation of microbial growth was carried out by adding the inoculum to a well containing only MHB. Sterility of the culture medium was confirmed by incubation in the assay plate. Assays were performed in 96-well microplates, in triplicate. The microplates were incubated at 37 °C for 24 h. As an indicator of microbial growth, 20 µL of 2,3,5-triphenyltetrazolium chloride (TTC) at 5 mg/mL were added to each well. The plates were incubated at 37 °C for 3 h. Then the TTC was solubilized with 100 µL of sodium lauryl sulfate solution in isopropanol 7 µg/mL and measured in a microplate reader at 485 nm. The result was expressed as the percentage of inhibition of the extracts in comparison with the microbial growth control, according to Fukuda *et al*. (2006). In the

present study, the extracts with inhibition higher than 50% were considered promising for further work, and the IC_{50} value was determined. Additionally, the minimal inhibitory concentration (MIC) of the extracts was determined by the microdilution assay in MHB (CLSI, 2003). The extracts solubilized in DMSO at 50 mg/mL were diluted in Mueller Hinton Broth (MHB) at concentrations of 2.0 mg/mL, 1.0 mg/mL, 500 µg/mL, 250 µg/mL, 125 µg/mL, 62.5 µg/mL and 31.25 µg/mL. The inoculums, controls, assemblage of the plate, incubation and measurement of the results were performed as described above. The MIC value was defined as the lowest concentration of each extract, which inhibited 55% of the microbial growth.

Phytochemical screening

The phytochemical screening for detection of secondary metabolites in the extracts of leaves and branches of *A. subincanum* was performed by TLC according to Wagner and Bladt (2001). The conditions used are shown in Table 1.

Exploratory profile of the extracts by high-performance liquid chromatography (HPLC)

HPLC profiles of the extracts were recorded on an Agilent Technologies 1200 series, chromatographic system, composed of a binary pump, an auto sampler, a diode array detector (DAD) and a ChemStation data handling system (Agilent Technologies, USA). Samples were prepared at 5 mg/mL in MeOH, filtered through 0.45 µm PTFE membranes, and 10 µL were injected into the HPLC system. An Hypersil C-18 column (250 × 4.6 mm i.d., 5 µm) in combination with a Hypersil RP-18 guard column (4 mm × 4.6 mm i.d., 5 µm) was employed for the analysis. Elution was carried out using a

gradient of ultrapure water (A) and acetonitrile (B), both acidified with 0.1% formic acid, from 5 to 95% of B in 60 min, at a flow rate of 1 mL/min, 40°C and detection at 210 nm.

RESULTS AND DISCUSSIONS

The genus *Aspidosperma* is a source of biologically active indole alkaloids (Pereira *et al*. 2007) even though other classes of secondary metabolites have been reported (Estrada *et al*., 2015). The species *A. subincanum* Mart. has yielded many indole alkaloids with high structural diversity.

Aiming to develop a highly predictive ligand-based model of the anticholinesterase activity and to apply it to indole alkaloids we developed a new method that comprehends the use of a multi-conformational 3D pharmacophore fingerprint, machine learning modeling and the prediction of probable activity.

Traditionally, the multi-conformational 3D pharmacophore modeling approach was avoided due to the exponential complexity associated with the need to superimpose different conformations of each compound. The use of pharmacophore fingerprint speeds up the process since superimposition is not required. However, choosing just one conformation per compound would not be enough, thus, our approach was to concatenate the uni-conformational fingerprints into one multi-conformational fingerprint, called modal fingerprint (Fig. 2) (Shemetulskis *at al*., 1996), which is the union of all fingerprints. If one bit is lit in one fingerprint it will be lit in the modal fingerprint as well. With this procedure we could take advantage of the high speed of

calculation using a single vector for each compound and, at the same time, retains the information about the conformational dynamics of the modeled compounds.

The modeling and validation procedures used a variant of the well-known bootstrap aggregating approach (bagging), introduced by Breiman (1996). The overall idea was to build several independent models, and average their output. This procedure is known to avoid overfitting and minimize prediction errors (Novotarskyi *et al*., 2016). In our approach 30 independent models were produced through stratified random partition of the original dataset to produce two subsets, the training set and the validation set (Fig. 3). This repetition process allows not only to validate the modeling method but, also, generates sufficient information about the score distribution of active and inactive compounds that could be used to predict the activity probability. The modeling performance was assessed through the area under the ROC curve (AUC) using the average scores of active and inactive compounds, collected exclusively from validation sets. The SVM model showed an excellent AUC of 0.911 while the Naïve Bayes produced an AUC of 0.775, which can be considered to be a good one.

All indole alkaloids (**1**-**21**) and reference compounds (**22**-**28**) had their corresponding pharmacophore fingerprints subjected to all 30 SVM and Naïve Bayes models produced in the modeling phase, as preconized by bagging approach (Breiman, 1996). To make predictions about anticholinesterase inhibition the mean score of each compound over all independent models was compared with the mean score distributions of active and inactive compounds that appeared in the validation sets in the modeling procedure (Fig. 3). Thereby the average scores were converted into the probabilities of being active (Pa) or inactive (Pi) as described in the Material and Methods section. It is important to note

that there is no direct correlation between the quantitative biological activities and Pa or Pi or Pa-Pi values. All models developed in this work were qualitative, that is, based solely on classification of compounds as active or inactive.

Table 2 shows the results of predictions of AChE inhibition of *A. subincanum* alkaloids and compounds used as positive control. In the SVM prediction, almost all compounds showed Pa-Pi positive values, with a few close to zero within confidence intervals (compounds **8**, **15**, **16** and **18**). Most positive control compounds (**22**-**28**) showed high positive values. The alkaloids 3,4-dihydroolivacine (**11**), guatambuine (**12**) and N-methyl-olivacine (**13**), in this order, presented better positive values higher than rivastigmine (**27**) and galantamine (**28**) but lower than other positive control compounds.

On the other hand, Naïve Bayes prediction showed more spanned values of Pa-Pi, with values as high as 0.620 for uleine (**1**) and des-N-methyl-uleine (**2**) and as low as -0.247 for N-methyl-olivacine (**13**). The alkaloids ellipticine (**6**) and olivacine (**10**) also showed Pa-Pi negative values. The values for positive control compounds (**22**-**28**) were not as high as could be expected, with a maximum of 0.610 for tacrine (**25**), but showed a negative value of -0.110 for galantamine (**28**). All uleines and dasycarpidones (**1**-**5**) showed Pa-Pi values above 0.58, higher or equal to positive control compounds. The subicanandines C and E to G (**17**, **19**-**21**) showed values of Pa-Pi above 0.5.

A reasonable agreement could be noted between predictions made with SVM and Naïve Bayes modeling methods, despite the magnitude of scores. The most prominent disagreement was observed for N-methyl-olivacine (**13**) which presented one of the highest values of Pa-Pi with SVM but was the lowest with Naïve Bayes. Both methods

are much used in ligand-based virtual screening studies and their performance varied depending on datasets, fingerprints and biological activity (Lavecchia, 2015), but it is difficult to say which one is the best for our specific problem. From our experience (JCD Lopes, personal communication), although SVM typically showed better validation results, Naïve Bayes can be more predictive.

When both methods are taken together (last column of Table 2) it is possible to conclude that uleines are more prone to present strong inhibition of AChE. It is worth noting that the anticholinesterase inhibitory activity of uleine (**1**) which has been reported elsewhere (Seidl *et al*., 2010), strongly confirmed our findings. However, the results from this study suggested that beyond uleine (**1**) and related compounds, the olivacines 3,4-dihydroolivacine (**11**) and guatambuine (**12**), and the subincanadines C (**17**) and E (**19**) also have a high potential to show the same activity. Thus, all the results reported here encouraged us to evaluate whether the crude and the alkaloid-enriched extracts of *A. subincanum* presented anticholinesterase inhibitory activity.

The inhibition of AChE was evaluated using qualitative and quantitative methods. In the bioautographic assay (Marston *et al*., 2002) all the evaluated extracts showed inhibition halos with different intensities (Fig. 4). In the bioautographic method one can expect to obtain false-positive results and the interpretation of the plates varies considerably among different analysts (Seidl *et al*., 2010). For this reason, in order to confirm the preliminary results and to determine the percentage of inhibition as well as the IC_{50} value for the promising extracts, they were evaluated using a microplate quantitative assay (Ellman *et al*., 1961).

The absorbance background measurement was recorded to discard the inhibition of the chemical reaction between DTNB and thiocholine (Rhee *et al*., 2003). Among the tested extracts, the EtOH extract of branches and the alkaloid-enriched fractions of branches (DCM branches) and leaves (DCM leaves) were considered active (%I higher than 50% at 400 µg/mL) as shown in Table 3. The reference compounds physostigmine and galantamine showed %I of 90.0 ±1.0 and 88.85 ± 0.73, respectively, at 15.6 µg/mL. The IC_{50} values observed for the extracts were considerably higher than that obtained for galantamine (IC_{50} 0.003 ± 0.01 µg/mL), ranging from 77.88 ± 9.49 (DCM extract of branches) to 233.11 ± 12.50 (EtOH extract of branches) as shown in Table 3. The DCM extract of branches showed the best inhibition among the tested samples, with an IC_{50} value of 77.88 ± 9.49 µg/mL. Therefore, the results indicate that the evaluated extracts induced a moderate inhibition of the enzyme. It is important to mention that this results were obtained for crude extracts and fractions, which can explain the higher IC_{50} values observed when compared with the reference compounds.

The aforementioned results are consistent with our findings from *in silico* prediction in which some indole alkaloids from *A. subincanum* have shown a high probability of inhibiting acethylcholinesterase activity. For this reason, it is worth to further investigate these samples aiming the identification of AChE inhibitory compounds.

Several studies of the AChE inhibition of plant extracts with indole alkaloids have been reported (Houghton *et al*., 2006; Murray *et al*., 2013). Mathew and Subramanian (2014) evaluated the anticholinesterasic activity of twenty medicinal plants used in Ayuverdic medicine to treat cognitive disorders. The extract of *Rauwolfia serpentina* (Apocynaceae), a specie rich in indole alkaloids, showed the greatest inhibition against

AChE (IC_{50} 22.0 ± 4.9 µg/mL). The alkaloid extract from *Uncaria rhynchophylla* (Miq.) Jacks (Rubiaceae) strongly inhibited AChE activity (IC_{50} value of 5.4 ± 0.4 mg/mL). The isolated indole alkaloid geissoschizine methyl ether showed strong AChE inhibiting activity (3.7 ± 0.3 mg/mL) (Yang *et al*., 2012).

As mentioned before, the inhibition of AChE is an important strategic tool in the treatment of neurodegenerative diseases such as AD and Parkinson's disease (PD). However, there are other important components in the pathophysiology of neurodegenerative diseases, as for example, oxidative stress. Therefore, the antioxidant potential of the extracts of *A. subincanum* was also evaluated. The extracts were considered promising when they exhibited IC_{50} values lower than 50 µg/mL in the β-carotene bleaching assay and/or IC_{50} values lower than 15 µg/mL in the DPPH assay. The EtOH extract of branches was able to prevent the β-carotene bleaching (IC_{50} value of 39.0 ± 3.4 µg/mL) similarly to the effect induced by rutin (39.4 ± 1.6 µg/mL, Table 3). In contrast, none of the extracts showed a significant capacity to reduce the DPPH radical, since they exhibited IC_{50} values > 15 µg/mL in this assay (Table 3). Hence, the EtOH extract of branches from *A. subincanum* has the potential to inhibit oxidative stress related to lipid peroxidation but did not show a capacity for scavenging free radicals. In order to confirm its potential as a source of antioxidant compounds, further experiments should be performed.

It has been reported that plant extracts containing uleine have shown antimicrobial activity (Federlin *et al*., 2014). Therefore, we also evaluated the antimicrobial activity of the extracts of *A. subincanum*.

In the antibacterial susceptibility test, none of the extracts showed activity against the Gram-negative bacteria *E. coli.* For *S. aureus*, the ethanolic extracts demonstrated a discrete antibacterial activity in the microplate assay, ranging from 40.6 ± 9.6 (EtOH branches) to 69. 4 ± 4.4 (DCM branches) (Table 3). The EtOH extract of leaves showed an IC_{50} value of 221.04 ± 5.32, whereas the EtOH extract of branches had an inhibition lower than 50% and, hence, an IC_{50} value was not applicable. In contrast, the alkaloid-enriched extracts of branches and leaves showed promising antibacterial activity, with values of growth inhibition of 69.4% and 68.8%, respectively, at a concentration of 1.0 mg/mL and an IC_{50} values of 71.87 ± 9.33 (DCM branches) and 123.42 ± 38.47 (DCM leaves) µg/mL. The MIC's values of an EtOH extract of leaves was 500 µg/mL, while the values of the alkaloid-enriched extracts were 125 µg/mL (branches) and 250 µg/mL (leaves) for Gram-positive *S. aureus*.

The antimicrobial activity of alkaloid-enriched fractions of *Aspidosperma* species was previously reported. Oliveira and colleagues (2009) demonstrated the potential of stem bark alkaloid fractions of *A. ramiflorum* against *Bacillus subtillis, S. aureus* and *E. coli*, with MIC values of 31.5 mg/mL, 62.5 mg/mL and 250.0 mg/mL, respectively. Pessini *et al*. (2012) also presented a relevant antimicrobial activity of ethanolic extracts and alkaloid fractions of *A. tomentosum* and *A. pyrifolium* against *S. aureus*, *B. subtillis*, *Candida albicans*, *C. parapsilosis* and *C. tropicalis*, but no activity against *E. coli* and *P. aeruginosa*. Both authors corroborated the increased activity of alkaloid-enriched extracts and fractions against Gram-positive strains, which were also observed in this work.

According to the phytochemical screening performed with the leaves and branches of *A. subincanum* it was possible to detect the presence of steroids and triterpenoids, tannins, organic acids and alkaloids, while coumarins, anthracenic compounds, flavonoids and saponins were not detected. In our study, the inhibition of the enzyme acetylcholinesterase observed could be due to the presence of alkaloids even though other classes of metabolites were detected as aforementioned. Likewise, the computational studies demonstrated that some of them have a strong probability to inhibit the acetylcholinesterase enzyme. Moreover, the antioxidant activity observed in this study may be attributed to the phenolic compounds detected, since this correlation is well established (Gong *et al*., 2012). However, the isolation of this class of metabolites has not been described yet for *A. subincanum* based on the literature consulted.

The exploratory profile obtained by RP-HPLC showed constituents of different polarities in the alkaloid-enriched (DCM) and ethanolic extracts (Fig. 5). The presence of indole alkaloids was observed in all the evaluated extracts as well as triterpenes and steroids. The EtOH extract from leaves of *A. subincanum* (Fig. 5A) showed 4 major peaks for compounds of lower polarity (rt 41.29, 42.45, 51.13 and 55.16 min). The UV spectra of peaks 1 and 2 (rt 41.29 and 42.45 min) showed absorption bands characteristic of indole alkaloids (Sangster and Stuart, 1965), with λ_{max} of 310 nm. The UV spectra of peaks 3 and 4 showed absorption at λ_{max} of ca. 230 nm, indicative of less conjugated structures such as triterpenes and steroids. The alkaloid-enriched extract of leaves (Fig. 5B) presented 5 major peaks, one peak of higher polarity (peak 1, rt 15.25 min) with a UV spectrum showing an absorption band at λ_{max} of ca. 230 nm, and the 4 peaks observed in the chromatogram of the EtOH extract (rt 41.29, 42.45, 51.03 and

55.10 min). The UV spectrum of peaks 2 and 3 also showed absorption bands with λ_{max} of 310 nm similar to peaks 1 and 2, which were observed in the ethanolic extract from the leaves. The UV spectrum of peaks 1, 4 and 5 indicated less conjugated chromophore groups. Most of the constituents from the EtOH extract from branches (Fig. 5C) were eluted with retention times lower than 20 min, indicating substances of higher polarity. Three peaks of major intensity (rt 8.46, 12.16 and 15.91 min) were observed in this time scale. The UV spectrum of peaks 1 and 3 (λ_{max} of 240, 290 and 330 nm) showed absorption bands characteristic of indole alkaloids. The alkaloid-enriched extract of branches (Fig. 5D) revealed a more complex profile with 6 major peaks indicating the presence of compounds of different polarities. Only peak 1 showed absorption bands characteristic of indole alkaloids, with λ_{max} of 310 nm. The other peaks showed absorption bands at lower wavelenghts, indicative of less conjugated chromophores.

The chromatographic data suggests that the major constituents of the evaluated extracts are alkaloids and terpenes. In addition, other metabolites found in the leaves and branches of *A. subincanum,* such as phenolics, might also contribute to some extent to the antimicrobial, as well as antioxidant activities. In fact, some authors have extensively correlated the antioxidant and antibacterial activities to the phenolic content of samples (Allahghadri *et al.*, 2010; Silva *et al*., 2012, Rabêlo et *al.*, 2014).

In summary, among the evaluated samples the enriched-alkaloid extract of branches (DCM branches) demonstrated a better performance in the biological assays. It might be considered the most promising extract for further work regarding the search for compounds with anticholinesterase, antioxidant as well as antimicrobial activities. Moreover, the presence of alkaloids was detected in the extracts of branches and leaves

together with triterpenes and steroids. Furthermore, these classes of metabolites have several biological activities reported in the literature such as their anticholinesterasic, antioxidant and antimicrobial activity (Murray *et al*., 2013; Howes and Houghton, 2009; Cowan, 1999).

CONCLUSIONS

The present study showed that *A. subincanum* extracts have acetylcholinesterase inhibitory activity as well as antioxidant properties assessed by the lipid peroxidation assay and antimicrobial activity against *S. aureus* ATCC 25923. These activities might be differentiated by the chemical composition of the evaluated extracts although it needs further investigation. Our *in silico* results on the inhibition of acetylcholinesterase activity corroborated with earlier studies in which uleine (**1**) showed inhibition of this enzyme.

According to the *in silico* prediction of AChE inhibition, mainly the results of predictions made with Naïve Bayes models, showed that uleine and derivatives (**1**-**6**) have the highest probability to present anticholinesterase inhibitory activity, followed by 3,4-dihydroolivacine (**11**) and guatambuine (**12**) and subincanadines C (**17**) and E (**19**) which could be promising targets for anticholinesterase activity.

Our studies provide important results of the biological potential of *A. subincanum* with promising pharmacological action to be investigated in future research. These results can contribute to an increase in our knowledge of this species from the biodiversity of Brazil. Additionally, the outcome of this investigation may enable the opening of an

avenue to be explored towards the application of extracts and isolated compounds from *A. subincanum* as an alternative source for drug discovery.

CONFLICTS OF INTEREST

The authors of this manuscript declare no conflicts of interest.

ACKNOWLEDGMENTS

The authors are grateful to FAPEMIG for the financial support (Process Ref. DEG/AUC-43/10) and for the scholarship granted to MP Rocha and PRV Campana (BIP-0224-15), and to CNPq for the fellowship of VL Almeida (249299/2013-5) and JCD Lopes (202407/2014-4) in the Science Without Borders program. The authors also acknowledge AWA Linghorn for revising the English language in the manuscript.

REFERENCES

Albernaz LC, Paula JE, Romero GAS, Silva MRR, Grellier P, Mambu L, Espindola LS. 2010. Investigation of plants extracts in traditional medicine of the Brazilian Cerrado against protozoans and yeasts. *J Ethnopharmacol* **131**: 116-121.

Allahghadri T, Rasooli I, Owlia P, Nadooshan MJ, Ghazanfari T, Taghizadeh M, Astaneh SDA. 2010. Antimicrobial property, antioxidante capacity, and cytotoxicity of essential oil from Cumin produced in Iran. *J Food Sci* **75**(2): H54-H61.

Bhaskar M, Chintamaneni M. 2014. Investigating the role of *Eclipta alba* on brain antioxidant markers, cognitive performance and acetylcholinesterase activity of rats. *J Pharm Phytopharmacol Res* **3**(5): 390-394.

Bolton EE, Kim S, Bryant SH. 2011. PubChem3D: Conformer generation. *J. Cheminform* **3**(1): 4.

Brandão MGL, Grandi T, Rocha E, Sawer D, Krettli A. 1992. Survey of medicinal plants used as antimalarials in the Amazon. *J Ethnopharmacol* **36**: 175-182.

Breiman L. 1996. Bagging predictors. *Mach Learn* **24**(2): 123-140.

Chang C-C, Lin C-J. 2011. LIBSVM: a library for support vector machines. ACM Transactions on Intelligent Systems and Technology, 2:27:1-27:27. Software available at < http://www.csie.ntu.edu.tw/~cjlin/libsvm >.

CLSI. Clinical and Laboratory Standards Institute. 2003. Methods for dilution antimicrobial susceptibility tests for bacteria that grow aerobicall; Approved Standard - 6th Edition M7-A6, Pennsylvania: Clinical and Laboratory Standards Institute (CLSI), vol. **23**(2).

Cowan MM. 1999. Plant products as antimicrobial agents. *Clin Microbiol Rev* **12**(4): 564-582.

Cragg GM, Newman DJ. 2005. Plants as source of anticancer agents. *J Ethnopharmacol* **100**: 72-79.

DeLong ER, DeLong DM, Clarke-Pearson DL. 1988. Comparing the area under two or more correlated receiver operating characteristic curves: a nonparametric approach. *Biometrics* **44**: 837–845.

Domingues BF. 2012. 3D-Pharma: uma ferramenta para triagem virtual baseada em fingerprints de farmacóforos (Tese). Universidade Federal de Minas Gerais (UFMG). Available at http://www.bibliotecadigital.ufmg.br/dspace/handle/1843/BUBD-9DKHDA.

Duarte-Almeida JM, Santos RJ, Genovese MI, Lajolo FM. 2006. Avaliação da atividade antioxidante utilizando o sistema β-caroteno/ácido linoleico e método de sequestro de radicais DPPH. *Ciên Tecnol Aliment* **26**(2): 446-452.

Ellman GL, Courtney KD, Junior VA, Featherstone RM. 1961. A new and rapid colorimetric determination of acetylcholinesterase activity. *Biochem Pharmacol* **7**: 88-95.

Estrada O, González-Gusmán JM, Salazar-Bookman MM, Cardozo A, Lucena E, Alvarado-Castilho CP. 2015. Hypotensive and bradyeardie effects of quinovic acid glycosides from *Aspidosperma fendleri* in spontaneously hypertensive rats. *Nat Prod Comm* **10**(2): 281-284.

Federlin JD, Maes D, Maes R. 2014. *Aspidosperma subincanum* I. characterisation, extraction of an uleine-enriched fraction and potential health hazard due to the contaminant ellipticine. *Rev Bras Farmacogn* **24**: 293-297.

Filimonov DA, Lagunin AA, Gloriozova TA, Rudik AV, Druzhilovskii DS, Pogodin PV, Poroikov VV. 2014. Prediction of the biological activity spectra of organic compounds using the pass online web resource. *Chem Heterocycl Compd* **50**(3): 444-457.

Fukuda M, Ohkoshi E, Makino M, Fujimoto Y. 2006. Studies on the constituents of the leaves of *Baccharis dracunculifolia* (Asteraceae) and their cytotoxic activity. *Chem Pharm Bull* **54**(10): 1465-1468.

Giraldi M, Hanazaki N. 2010. Uso e conhecimento tradicional de plantas medicinais no Sertão do Ribeirão, Florianópolis, SC, Brasil. *Acta Bot Bras* **24**(2): 395-402.

Gong Y, Liu X, He WH, Xu HG, Yuan F, Gao YX. 2012. Investigation into the antioxidant activity and chemical composition of alcoholic extracts from defatted marigold (Tagetes erecta L.) residue. *Fitoterapia* **83**: 481–489.

Hawkins PCD, Nicholls A. 2012. Conformer Generation with OMEGA: Learning from the data set and the analysis of failures. *J Chem Inf Model* **52**: 2919-2936.

Hawkins PCD, Skillman AG, Warren GL, Ellingson BA, Stahl MT. 2010. Conformer generation with OMEGA: Algorithm and validation using high quality structures from the protein databank and Cambridge structural database. *J Chem Inf Model* **50**(4): 572-584.

Houghton PJ, Ren Y, Howes MJ. 2006. Acetylcholinesterase inhibitors from plants and fungi. *Nat Prod Rep* **23**: 181-199.

Howes MJ, Houghton PJ. 2009. Acetylcholinesterase inhibitors of natural origin. *Int J Biomed Pharmaceut Sci* **3**(Special issue 1): 67-86.

The Comprehensive Perl Archive Network (CPAN). Available in <http://search.cpan.org/perldoc?Algorithm%3A%3ANaiveBayes>. Accessed in 09/19/2017

JChem Base 16.8.22. 2016. ChemAxon available in <http://www.chemaxon.com>

Kobayashi J, Sekiguchi M, Shimamoto S, Shigemori H, Ishiyama H, Ohsaki A. 2002. Subincanadines A-C, novel quaternary indole alkaloids from *Aspidosperma subincanum*. *J Org Chem* **67**(18): 6449-6455.

Lavecchia A. 2015. Machine-learning approaches in drug discovery: methods and applications. *Drug Discov Today* **20**(3): 318-31.

Lopes JCD, Dos Santos FM, Martins-José A, Augustyns K, De Winter H. 2017. The power metric: a new statistically robust enrichment-type metric for virtual screening applications with early recovery capability. *J Cheminform* **9**: 7.

Marston A, Kissling J, Hostettmann K. 2002. A rapid TLC bioautography method for the detection of acetylcholinesterase and butyrylcholinesterase inhibitors in plants. *J Pharm Anal* **13**(1): 51-54.

Marvin 16.8.22. 2016. ChemAxon available in <http://www.chemaxon.com>

Mathew M, Subramanian S. 2014. In vitro screening for anti-cholinesterase and antioxidant activity of methanolic extracts of Ayurvedic medicinal plants used for cognitive disorders. *PLoS ONE* **9**(1): e86804.

Murray AP, Faraoni MB, Castro MJ, Alza NP, Cavallaro V. 2013. Natural AChE inhibitors from plants and their contribution to Alzheimer's disease therapy. *Curr Neuropharmacol* **11**(4): 388-413.

Mensor LL, Menezes FS, Leitão GG, Reis AS, Santos TC, Coube CS, Leitão SG. 2001. Screnning of Brazilian plant extracts for antioxidant activity by the use of DPPH free radical method. *Phytother Res* **15**: 127-130.

Nicholls A. 2014. Confidence limits, error bars and method comparison in molecular modeling. Part 1: The calculation of confidence intervals. *J Compt Aided Mol Des* **28**(9): 887-918.

Novotarskyi S, Abdelaziz A, Sushko Y, Körner R, Vogt J, Tetko IV. 2016. ToxCast EPA in vitro to in vivo challenge: Insight into the Rank-I Model. *Chem Res Toxicol* **29**(5): 768-75.

Oliveira AJB, Koike L, Reis FAM, Eguchi SY, Endo EH, Nakamura CV, Filho BPD. 2009. Preliminary studies on the antibacterial activity of crude extracts and alkaloids from species of *Aspidosperma. Pharma Biol* **47**(11): 1085-1089.

Omar SH, Scott CJ, Hamlin AS, Obied HK. 2017. The protective role of plant biophenols in mechanisms of Alzheimer's disease. *J Nutr Biochem* **47**: 1-20.

OMEGA 2.5.1.4: OpenEye Scientific Software, Santa Fe, NM. http://www.eyesopen.com. Hawkins PCD, Skillman AG, Warren GL, Ellingson BA, Stahl MT.

Paula RC, Dolabela MF, Oliveira AB. 2014. *Aspidosperma* species as sources of antimalarials. Part III. A review of traditional use and antimalarial activity. *Planta Med* **80**: 378-386.

Pereira MM, Jácome RLRP, Alcântara AFC, Alves RB, Raslan DS. 2007. Alcalóides indólicos isolados de espécies do gênero *Aspidosperma* (Apocynaceae). *Quim Nova* **30**(4): 970-983.

Perry E, Howes M-JR. 2011. Medicinal plants and dementia therapy: herbal hopes for brain aging? *CNS Neurosci Ther* **17**(6): 683-698.

Pessini GL, Aquino PGV, Bernardo VB, Costa MA, Nakamura CV, Ribeiro EAN, Sant'Ana AEG, Araújo-Júnior JX. 2012. Evaluation of antimicrobial activity of three Aspidosperma species. *Pharmacologyonline* **1**(Special issue): 112-119.

Rabêlo SV, Costa MM, Libório RC, Almeida JRGS. 2014. Atividade antioxidante e antimicrobiana de extratos de atemoia (*Annona cherimola* Mill. x A. *squamosa* L.). *Rev Bras Frutic* **36**: 265-271.

Rhee IK, van Rijn RM, Verpoorte R. 2003. Qualitative determination of false-positive effects in the acetylcholinesterase assay using thin layer chromatography. *Phytochem Anal* **14**(3): 127–131.

Sangster AW, Stuart KL. 1965. Ultraviolet spectra of alkaloids. *Chem Rev* **65**: 69-130.

Santos FM, De Winter H, Augustyns K, Lopes JCD. 2015. Use of extensive cross-validation and bootstrap application (ExCVBA) for molecular modeling of some pharmacokinetics properties. Poster presented at OPENTOX EURO 2015 - OpenTox InterAction Meeting - Innovation in Predictive Toxicology, Dublin, Ireland. DOI: 10.13140/RG.2.1.2274.8888.

Seidl C, Correia BL, Stinghen AEM, Santos AMC. 2010. Acetylcholinesterase inhibitory activity of uleine from *Himantanthus lancifolius*. *Z Naturforsch* **65c**: 440-444.

Shemetulskis NE, Weininger D, Blankley CJ, Yang JJ, Humblet C. 1996. Stigmata: an algorithm to determine structural commonalities in diverse datasets. *J Chem Inf Comput Sci* **36**(4): 862-871.

Silva MJD, Endo LH, Dias ALT, Silva GA, Santos MH, Silva MA. 2012. Avaliação da atividade antioxidante e antimicrobiana dos extratos e frações orgânicas de *Mimosa caesalpiniifolia* Benth. (Mimosa). *Ciênc Farm Básica Apli* **33**(2): 267-274.

Silva NCC, Fernandes Júnior A. 2010. Biological properties of medicinal plants: a review of their antimicrobial activity. *J Venom Anim Toxins incl Trop Dis* **16**(3): 402-413.

Stiborová M, Frei E. 2015. Ellipticines as DNA-targeted chemotherapeutics. *Curr Med Chem* 21(5): 575-591.

Tratado de Cooperación Amazonica (TCA). Plantas medicinales Amazónicas: realidade y perspectivas. Ediciones TCA. Lima: Ediciones TCA, 1995.

Yang Z, Duan D, Du J, Yang MJ, Li S, Yao X. 2012. Geissoschizine methyl ether, a corynanthean-type indole alkaloid from *Uncaria rhynchophylla* as a potential acetylcholinesterase inhibitor. *Nat Prod Res* **26**(1): 22–28.

Wagner H, Bladt S. 2001. *Plant Drug Analysis*: *A Thin Layer Chromatography Atlas* (2nd edn). Springer-Verlag: Berlin Heidelberg.

Wang Y, Bryant SH, Cheng T, Wang J, Gindulyte A, Shoemaker BA, Thiessen PA, He S, Zhang J. 2017. PubChem BioAssay: 2017 update. *Nucleic Acids Res* **45**(D1): D955-D963.

Ward JH. 1963. Hierarchical grouping to optimize an objective function. *J Am Statist Assoc* **58**: 236-244.

Table 1. Chromatographic conditions used in phytochemical screening by TLC

Class of secondary metabolites	Eluent	Spray reagent	Reference sample
Triterpenes and steroids	Ethyl acetate:hexane (10:10)	Anisaldehyde-sulphuric acid reagent	Lupeol
Tannins	Toluene:butanol:acetic acid:water (50:25:25:5)	$K_3Fe(CN)_6$ 1%: $FeCl_3$ 2% (1:1)	Tannic acid
Coumarins	Toluene:ethyl ether (1:1) saturated with glacial acetic acid	KOH reagent (5%)	*Brosimum gaudichaudii*
Anthracenic compounds	Ethyl acetate:methanol:water (81:11:8)	KOH reagent (5%)	*Cassia angustifolia*
Saponins	Chloroform:acetic acid:methanol:water (64:32:12:8)	Anisaldehyde-sulphuric acid reagent	*Centella asiatica* Escin
Flavonoids	Ethyl acetate:formic acid:acetic acid:water (100:11:11:27)	NP/PEG	Rutin; caffeic acid; chlorogenic acid
Alkaloids	Ethyl acetate:methanol:water (20:2:2)	Dragendorff reagent	Quinine

Table 2. Prediction of anticholinesterase activity for 21 indole alkaloids (**1**-**21**) isolated from *A. subincanum*, and some positive controls compounds (**22**-**28**) widely used in the anticholinesterase activity measurements. The models used to make the predictions are based on SVM and Naïve Bayes methods using 3D multi-conformational pharmacophore fingerprints. Values of Pa–Pi correspond to the difference between the probability of being active and the probability of being inactive (see Experimental Section for details of calculations). The Pa–Pi confidence intervals were analytically estimated at 95% confidence level according to Eq. 4. The ranking of each indole alkaloid compound within each model is also presented, as well as the relative position of each compound based on its average rank.

		SVM		Naïve Bayes		Relative Position
ID	Compounds	Pa - Pi	Rank	Pa - Pi	Rank	
1	Uleine	0.297 ± 0.082	11	0.620 ± 0.081	1	4
2	des-N-Methyluleine	0.237 ± 0.080	15	0.620 ± 0.081	1	6
3	epi-Uleine	0.250 ± 0.080	14	0.593 ± 0.082	5	8
4	Dasycarpidone	0.237 ± 0.080	15	0.603 ± 0.081	4	8
5	epi-Dasycarpidone	0.160 ± 0.075	18	0.583 ± 0.083	7	15
6	Ellipticine	0.160 ± 0.075	18	-0.237 ± 0.084	26	24
7	1,2-Dihydroellipticine	0.260 ± 0.081	12	0.267 ± 0.090	18	18
8	N-methyl-1,2-dihydroellipticine	0.007 ± 0.068	27	0.020 ± 0.088	24	28
9	N-methyl-tetrahydroellipticine	0.260 ± 0.081	12	0.267 ± 0.090	18	18
10	Olivacine	0.120 ± 0.076	22	-0.237 ± 0.084	26	27
11	3,4-Dihydroolivacine	0.393 ± 0.084	6	0.353 ± 0.090	14	10
12	Guatambuine	0.360 ± 0.083	7	0.370 ± 0.090	13	10

13	N-methyl-olivacine	0.350 ± 0.083	8	-0.247 ± 0.083	28	20
14	1,2-dihydropyridocarbazol	0.160 ± 0.075	18	0.083 ± 0.089	23	22
15	Subincanadine A	-0.007 ± 0.069	28	0.280 ± 0.090	15	23
16	Subincanadine B	0.010 ± 0.068	26	0.280 ± 0.090	15	22
17	Subincanadine C	0.227 ± 0.079	17	0.583 ± 0.083	7	12
18	Subincanadine D	0.080 ± 0.073	25	0.170 ± 0.090	21	25
19	Subincanadine E	0.320 ± 0.083	10	0.500 ± 0.086	11	11
20	Subincanadine F	0.113 ± 0.076	24	0.500 ± 0.086	11	19
21	Subincanadine G	0.160 ± 0.075	18	0.583 ± 0.083	7	15
22	Physostigmine	0.500 ± 0.084	2	0.157 ± 0.090	10	4
23	Donepezil	0.900 ± 0.050	3	0.280 ± 0.090	3	1
24	7-Methoxytacrine	0.633 ± 0.080	1	0.547 ± 0.084	15	6
25	Tacrine	0.500 ± 0.084	5	0.610 ± 0.081	5	2
26	Huperzine A	0.477 ± 0.085	3	0.593 ± 0.082	22	15
27	Rivastigmine	0.350 ± 0.083	8	0.183 ± 0.090	20	16
28	Galantamine	0.120 ± 0.076	22	-0.110 ± 0.087	25	26

Table 3. Anticholinesterase, antioxidant and antibacterial activities of EtOH and alkaloid-enriched extracts of *A. subincanum*

Samples	Inhibition of AChE (25 – 400 µg/mL)			Antioxidant activity (6,25 – 200 µg/mL)		Antibacterial activity (12,5 – 500 µg/mL)		
	TLC	% I ± SD (400 µg/mL)	IC_{50} (µg/mL) ± SD	Lipid peroxidation IC_{50} (µg/mL)	DPPH assay IC_{50} (µg/mL)	% I ± SD (500 µg/mL)	MIC 55% (µg/mL) *S. aureus*	IC_{50} (µg/mL) *S. aureus*
EtOH branches	++++	56.0 ± 3.7	233.11 ± 12.50	39.0 ± 3.4	99.4 ± 0.8	40.6 ± 9.6	NT	NT
EtOH leaves	++++	38.7 ± 3.3	NT	61.7 ± 9.5	161.8 ± 42.1	56.3 ± 10.6	500	221.04 ± 5.32
DCM branches	+	63.6 ± 8.7	77.88 ± 9.49	NT	NT	69.4 ± 4.4	125	71.87 ± 9.33
DCM leaves	++	68.7 ± 4.4	185.43 ± 24.37	NT	NT	68.8 ± 7.8	250	123.42 ± 38.47
Physostigmine (15.6 µg/mL)	++++	90.0 ± 1.0	NT	NA	NA	NA	NA	NA
Galantamine (15.6 µg/mL)	NT	88.85 ± 0.73	0.03 ± 0.01	NA	NA	NA	NA	NA
Quercetin	NA	NA	NA	0.3 ± 0.1	NA	NA	NA	NA
Rutin	NA	NA	NA	39.4 ± 1.6	NA	NA	NA	NA
Pyrogallol	NA	NA	NA	NA	1.1 ± 0.1	NA	NA	NA
Chloramphenicol (50 µg/mL)	NA	NA	NA	NA	NA	100.0	NT	NT

(+) less active; (++) fairly active; (++++) very active. EtOH: ethanol extract; DCM: alkaloid-enriched extract. NA: not applicable; NT: not tested.

Figure Captions

Figure 1. Chemical structures of indole alkaloids isolated from *Aspidosperma subincanum* as reported in the literature (Pereira *et al*., 2007).

Figure 2. Generation of multi-conformational pharmacophore fingerprint using in-house 3D-Pharma software (Domingues, 2012). From the 2D structure of the compound of interest (uleine in the example above) up to 10 conformations are generated. For each conformation, pharmacophore points are calculated for all heavy atoms in the 3D space. All combinations of 3-points correspond to one pharmacophore triplet which is associate to one bit in the fingerprint vector. The modal fingerprint which holds all information about the conformations is the union of uni-conformational fingerprints.

Figure 3. AChE inhibition modeling and prediction. The whole procedure of AChE inhibition modeling and prediction involves four separated steps: dataset preparation, machine learning modeling, model validation and prediction. The multi-conformational modal pharmacophore fingerprints of all compounds were submitted to modeling pipeline with SVM and Naïve Bayes machine learning methods. The ROC curve was built with the mean score of each compound when it appears in the validation set. The mean score of unseen compounds is compared to the mean score distribution of active and inactive compounds to evaluate its probability of belonging to one or other group, as shown in the upper right graphic pane as vertical colored lines for olivacine (solid line), uleine (dotted line) and physostigmine (dashed line). The result of the prediction is the difference between the probability of being active (Pa) and the probability of being inactive (Pi) as shown in the lower right graphic pane for compounds olivacine (solid line), uleine (dotted line) and physostigmine (dashed line).

Figure 4. TLC bioautograph assay showing the inhibition of acetylcholinesterase activity by extracts (20 mg/mL) of *A. subincanum.* 1: Ethanolic extract of branches; 2: Alkaloid-enriched extract of branches; 3: Ethanolic extract of leaves; 4: Alkaloid-enriched extract of leaves; 5: Physostigmine (positive control). Solvent system: Chloroform:methanol (9:1). Spray reagent: Solution of 1-naphythyl acetate and Fast Blue B salt. See the assay conditions on the Material and Methods section. White spots indicate the inhibition zones on a purple background.

Figure 5. Profiles obtained by RP-HPLC of ethanolic extracts and alkaloid-enriched extract of *A. subincanum.* A: Ethanolic extract of leaves; B: Alkaloid-enriched extract of leaves; C: Ethanolic extract of of branches; D: Alkaloid-enriched extract of branches.

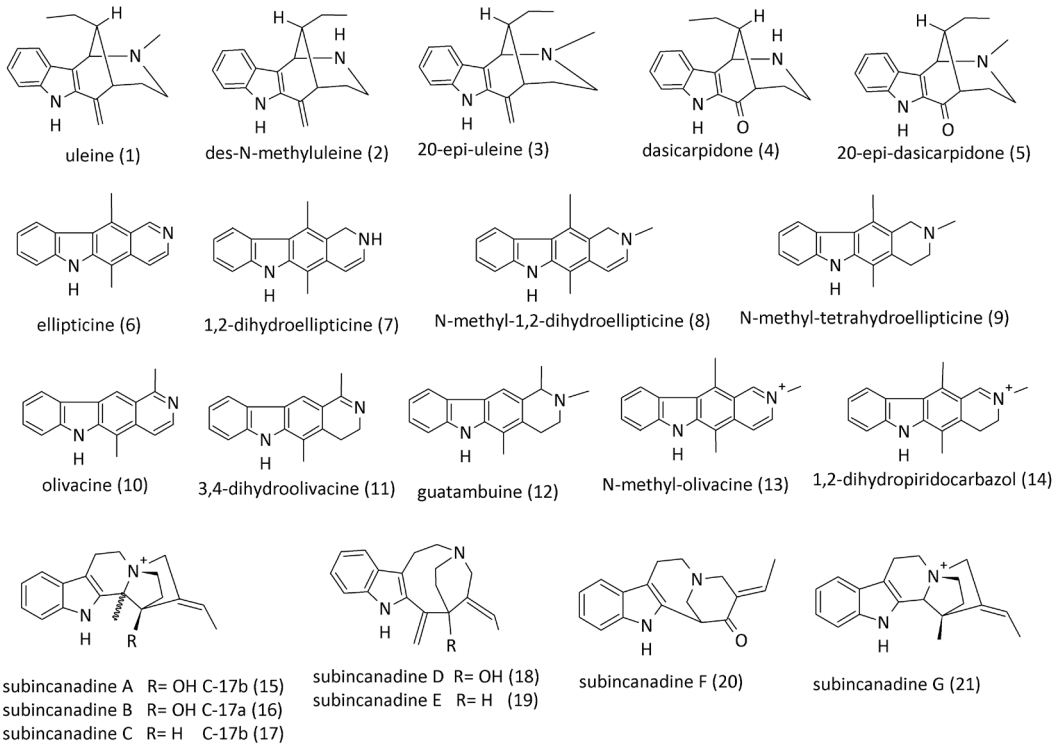

Figure 1

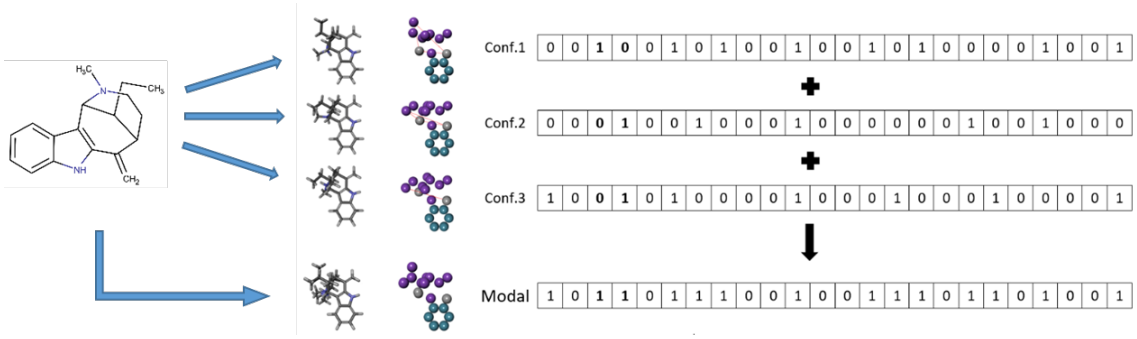

Figure 2

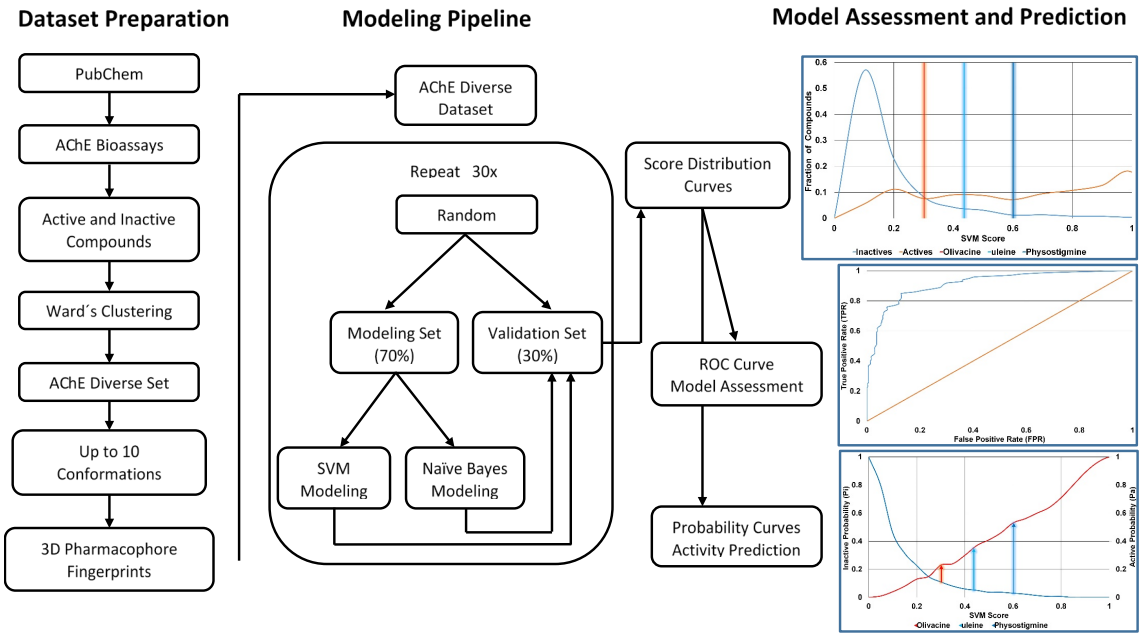

Figure 3

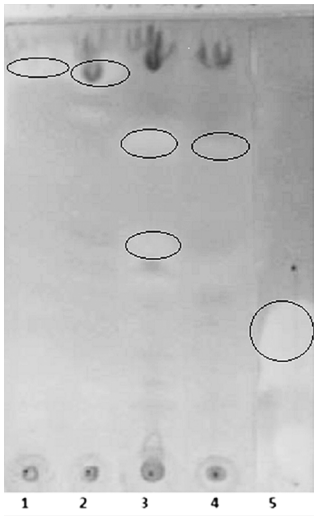

Figure 4

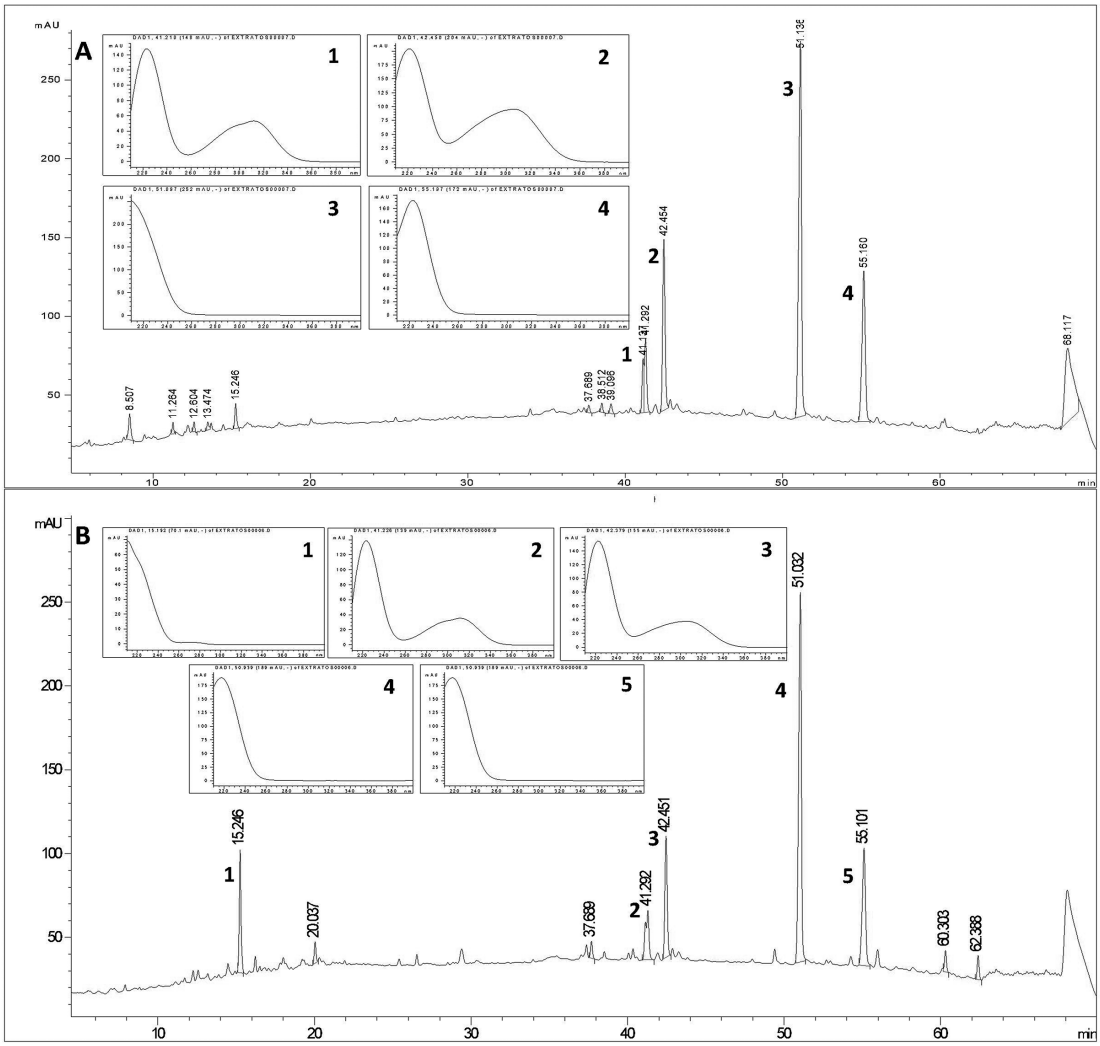
A
mAU
1
2
3
4
8.507
11.264
12.604
13.474
15.246
37.689
38.512
38.966
41.292
42.454
51.135
55.160
68.117
min
B
mAU
1
2
3
4
5
15.246
20.037
37.689
41.292
42.451
51.032
55.101
60.303
62.388
min

Figure 5 A-B

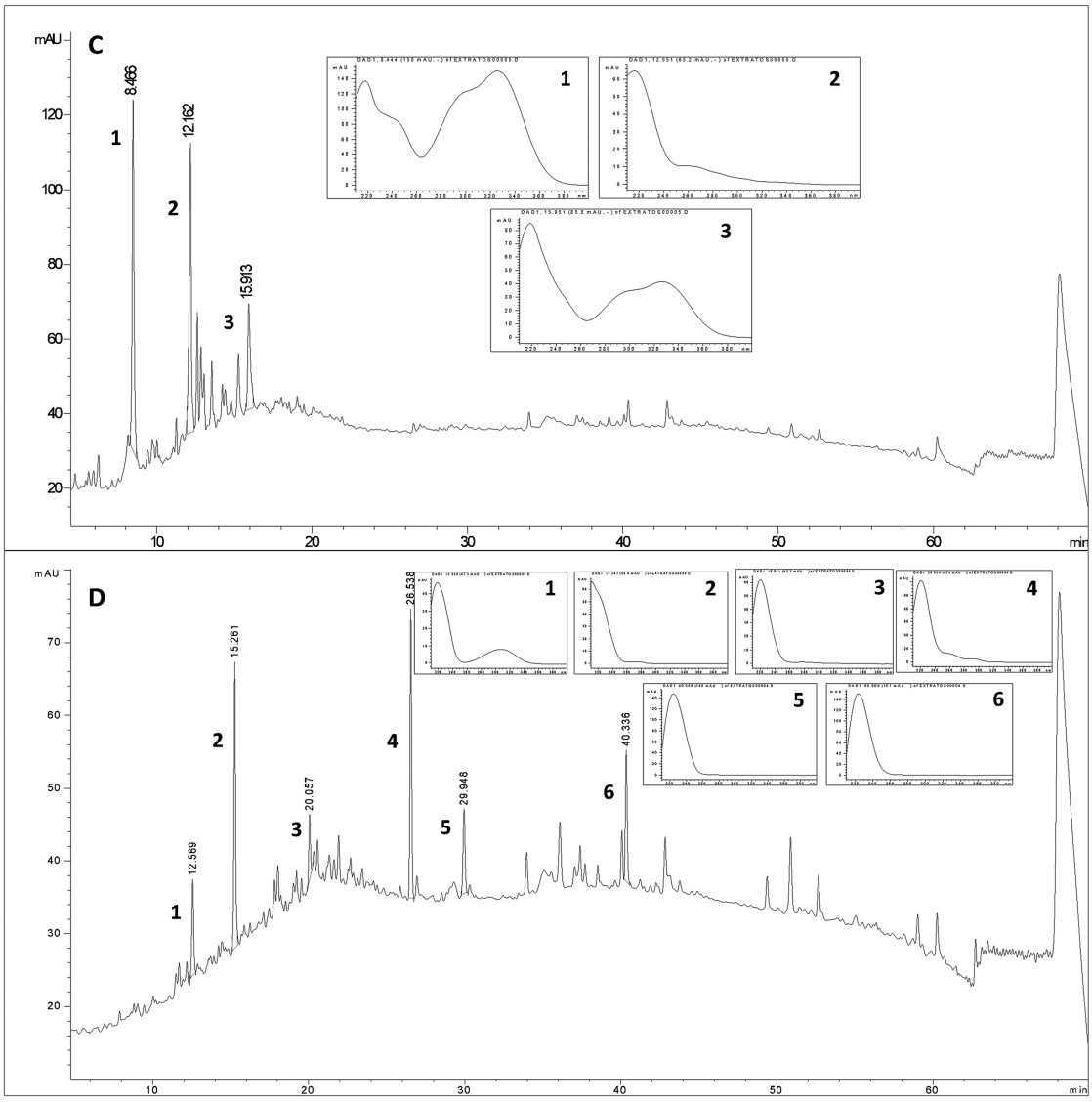
C
mAU
8.466
12.162
15.913
1
2
3
min
D
12.569
15.261
20.057
26.538
29.946
40.336
4
5
6

Figure 5 C-D